This is the post-print (i.e. final draft post-refereeing) of the publication.
The final publication is available at Elsevier via https://doi.org/10.1016/j.materresbull.2021.111311

Toward a new PTCR material based on the $Na_2Ti_6O_{13}/Na_2Ti_3O_7$ system

L. A. L. Basilio[a], J. H. L. Silva[b], F. Xavier[c], L. Aguilera[c], F. Guerrero[d], E. Antonelli[e], J. Anglada-Rivera[f], J. E. Garcia[g], R. S. Silva[b], Y. Leyet[a,d]

[a]*LPMaT, Programa de Pós-graduação em Ciência e Engenharia de Materiais, Departamento de Engenharia de Materiais, Universidade Federal do Amazonas, Manaus, Amazonas, Brasil*

[b]*Departamento de Física, Universidade Federal de Sergipe, Aracaju, Sergipe, Brasil*

[c]*Programa de Pós-graduação em Química, Departamento de Química, Universidade Federal do Amazonas, Manaus, Amazonas, Brasil*

[d] *Programa de Pós-graduação em Física, Departamento de Física, Universidade Federal do Amazonas, Manaus, Amazonas, Brasil*

[e]*Advanced Ceramic Laboratory, Science and Technology Institute, Universidade Federal de São Paulo, São José dos Campos, SP, Brasil*

[f]*Instituto Federal de Educação, Ciência e Tecnologia do Amazonas, Manaus, Amazonas, Brasil*

[g]*Department of Physics, Universitat Politècnica de Catalunya – BarcelonaTech, Barcelona, Spain*

Contact: Y. Leyet - yurileyet@yahoo.es

Abstract

Mixed phases of sodium titanate ceramics are obtained using both conventional and laser sintering methods. It was observed a clear dependence on the structural, microstructural and electrical resistivity with the employed sintering method. The temperature dependence of the resistivity in the ceramics shows an increase of three orders of magnitude in a narrow range of temperatures, thereby indicating a noticeable positive temperature coefficient of resistivity (PTCR) effect. To explain this observed abnormal behavior, a model based on the structure of the $Na_2Ti_6O_{13}/Na_2Ti_3O_7$ composite is proposed. A new class of PTCR materials is reported.

Keywords: sodium titanate, laser sintering, resistivity, PTCR

Introduction

Materials belonging to the $Na_2Ti_nO_{2n+1}$ family have aroused considerable interest in the scientific and technological community owing to their potential use in energy technologies [1]. Several researchers have investigated this family in the powder form [2–8] and as films [9] and ceramics [10-12]. $Na_2Ti_3O_7$ and $Na_2Ti_6O_{13}$ stand out as the most important phases of this family and both compositions presented monoclinic structure with different space groups, i.e., P21/m and C2/m, respectively [13]. $Na_2Ti_3O_7$ exhibits a layers structure while $Na_2Ti_6O_{13}$ has tunnels that favor the ionic conduction [14,15]. It was found that their physical and chemical properties are heavily dependent on the processing conditions [16]. Recently, the synthesis of $Na_2Ti_3O_7/Na_2Ti_6O_{13}$ composite using the sonochemical method was reported for the first time [3,11]. The authors observed the formation of fine particles (8–20 nm) and, after sintering, the ceramics exhibited DC conductivity values of 10^{-6} $S{\cdot}cm^{-1}$ and a low relative density (<80%) [11,15,17].

Recently, a new laser sintering method, in which a CO_2 laser is used as the heating source, was proposed. This method is characterized by less costs, use of very high heating and cooling rates, and promote the rapid densification of several oxides, such as $BaTiO_3$ [18], YAG [19], $Ba_{1-x}Ca_xTiO_3$ [20] and $CaCu_3Ti_4O_{12}$ [21]. In some cases, the laser-sintered ceramics also exhibit better physicochemical properties when compared with conventionally sintered [18–21].

Some polycrystalline materials, such as doped $BaTiO_3$, can exhibit an unusual resistivity response (PTCR effect) as temperature function. In $BaTiO_3$, this behavior is because a potential barrier is formed at Curie temperature, which hinders the mobility of charge carriers. The origin of this potential barrier can be related to the formation of structural defects during the fabrication process [22,23]. $Na_2Ti_3O_7/Na_2Ti_6O_{13}$ ceramics show better charge mobility and electrical conductivity than those with single phases [8,13]. This

is attributed to the peculiar structural characteristics of these crystalline phases. $Na_2Ti_3O_7$ exhibits an open structure; hence, it shows a good ion exchange capacity without losing its lamellar structure, yielding a high density of charge carriers [24]. Moreover, in the $Na_2Ti_6O_{13}$ phase, the oxygen atoms are coordinated by at least two titanium atoms, creating a structure in the form of tunnels, which can function as conducting paths [24]. Recently, the semiconductor characteristics of ceramic samples with a pure $Na_2Ti_6O_{13}$ phase synthesized using the sonochemical method have been reported, indicating the presence of p-type charge carriers at room temperature [14]. However, the $Na_2Ti_3O_7/Na_2Ti_6O_{13}$ composite have scarcely been studied, particularly how the electrical properties of theses mixed phases depend on the temperature. In this work, the evidence of a new PTCR material based on the $Na_2Ti_6O_{13}/Na_2Ti_3O_7$ system is presented. The ceramics were sintered using both conventional and laser sintering methods, and the structural, microstructural and electrical properties were analyzed. Consequently, a new PTCR material is obtained with easily tunable properties that depended on its structure and/or microstructure.

Materials and methods

$Na_2Ti_6O_{13}/Na_2Ti_3O_7$ powders were synthesized by sonochemical method. Sodium hydroxide (NaOH, Merck, 99%) and titanium isopropoxide ($C_{12}H_{28}O_4Ti$, Aldrich, 97%) were used as precursor materials. NaOH was dissolved in isopropyl alcohol and ultrapure water. Separately, $C_{12}H_{28}O_4Ti$ was dissolved in isopropyl alcohol, and it was slowly added to the NaOH solution to avoid a sudden precipitation of TiO_2. Thereafter, the solution was subjected to ultrasound irradiation for 60 min at 500 W under a continuous pulse using the ECO-SONICS model QR750 [8, 14]. The powder was dried at 100 °C for 6 h and then uniaxially conformed in the disk form. Note that no washing process was performed to retain the same proportion of used reagents. The sintering process was performed using two

methods: conventional and laser sintering. Conventional sintering was conducted in an electric furnace at 1100°C for 2 h. Laser processing was performed using a CO_2 laser (GEM-100L–Coherent) operating in continuous mode, as described in the following. Initially, the sample was placed on a hot plate preheated at 200°C. Then, the CO_2 laser beam was expanded and guided to the center of the sample, where the diameter was 4.6 ± 0.5 mm. The laser power was increased up to a density of 0.28 W/mm^2 at a linear power rate of 0.01 W/mm^{2}s and kept constant for 15 s. This first stage of the sintering was performed to decrease the thermal gradient of the sample, which inhibits the formation of cracks, and remove the organic binder. Next, the laser power was further increased to a maximum density of 1.1 W/mm^2 at 0.03 W/mm^{2}s and held for 120 s. The laser power source was then turned off, and the entire process was repeated at the other sample surface. This entire procedure was repeated to ensure sintering efficiency and homogeneity along the thickness of the entire sample, and the total processing time was 7 min. The selected power density achieves a temperature of approximately 1100°C, which was measured using a type S thermocouple (0.25-mm diameter) placed on the sample surface during sintering [21]. The conventional and laser-sintered samples are referred to as NTF and NTL, respectively.

X-ray diffraction (XRD) patterns of each sample were collected using a Bruker X-ray diffractometer, Advance D8 model, in a 2θ range of 5°–80° (Cu-Kα, λ = 0.15406 nm) with a step size of 0.021° min^{-1}. The Rietveld refinement was performed using the GSAS software. The surface morphology of the samples was examined using scanning electron microscopy (SEM) by employing the Jeol microscope (JSM-6510LV model). The Archimedes method was used to determine the sample density.

For electrical characterization, silver electrodes were brushed to the polished surfaces of the ceramics and then dried at 300°C for 30 min. A Solartron 1260 Impedance Analyzer coupled with a 1296A dielectric interface was used to collect the impedance data in the

frequency range of 1–10^6 Hz. The measurements were performed using an alternating voltage of 500 mV from 25°C to 250°C.

Results and discussion

NTF and NTL ceramics achieved densities of 2.8 and 3.2 g·cm^{-3}, respectively. The density of NTL showed an improvement of approximately 10%. This observation can be attributed to the high heating rates in laser sintering, which decrease the activation energies in the initial stage of sintering [16], promoting high densities.

Figure 1 shows the structural Rietveld refinement plot of the XRD patterns and SEM images of both NTF (Figs. 1a and c) and NTL (Figs. 1b and d) samples. The refinement was performed using the experimental XRD pattern, and the inorganic crystal structure database card nos. 23877 ($Na_2Ti_6O_{13}$) and 15463 ($Na_2Ti_3O_7$) were used as references. The peak profile was modeled using the pseudo-Voigt function. The unit cell parameters, atomic positions, sample displacement, Lorentz coefficient, and the asymmetry of the diffraction peaks were also refined. The results verified the good correlation between the experimental and theoretical intensities for both samples (Fig. 1a and b), as observed in the residual line. The Rietveld refinement results are summarized in Tables S1–S6 (Supplemental Material). The phase composition analysis revealed that $Na_2Ti_6O_{13}$ was the major phase at 84% ± 1% and 86% ± 1% in NTF and NTL, respectively, while $Na_2Ti_3O_7$ was the secondary phase at 16% ± 1% and 14% ± 1% in NTF and NTL, respectively. The SEM images (Figure 1c and d) revealed several elongated rod-like grains with homogeneous morphology. However, NTL showed a larger grain size than NTF. The grain growth mainly occurs in the final stage of sintering owing to grain boundary migration and closed residual pores [13].The larger grain size of the laser-sintered ceramic indicates that the diffusion processes had occurred and/or higher sintering temperatures were achieved.

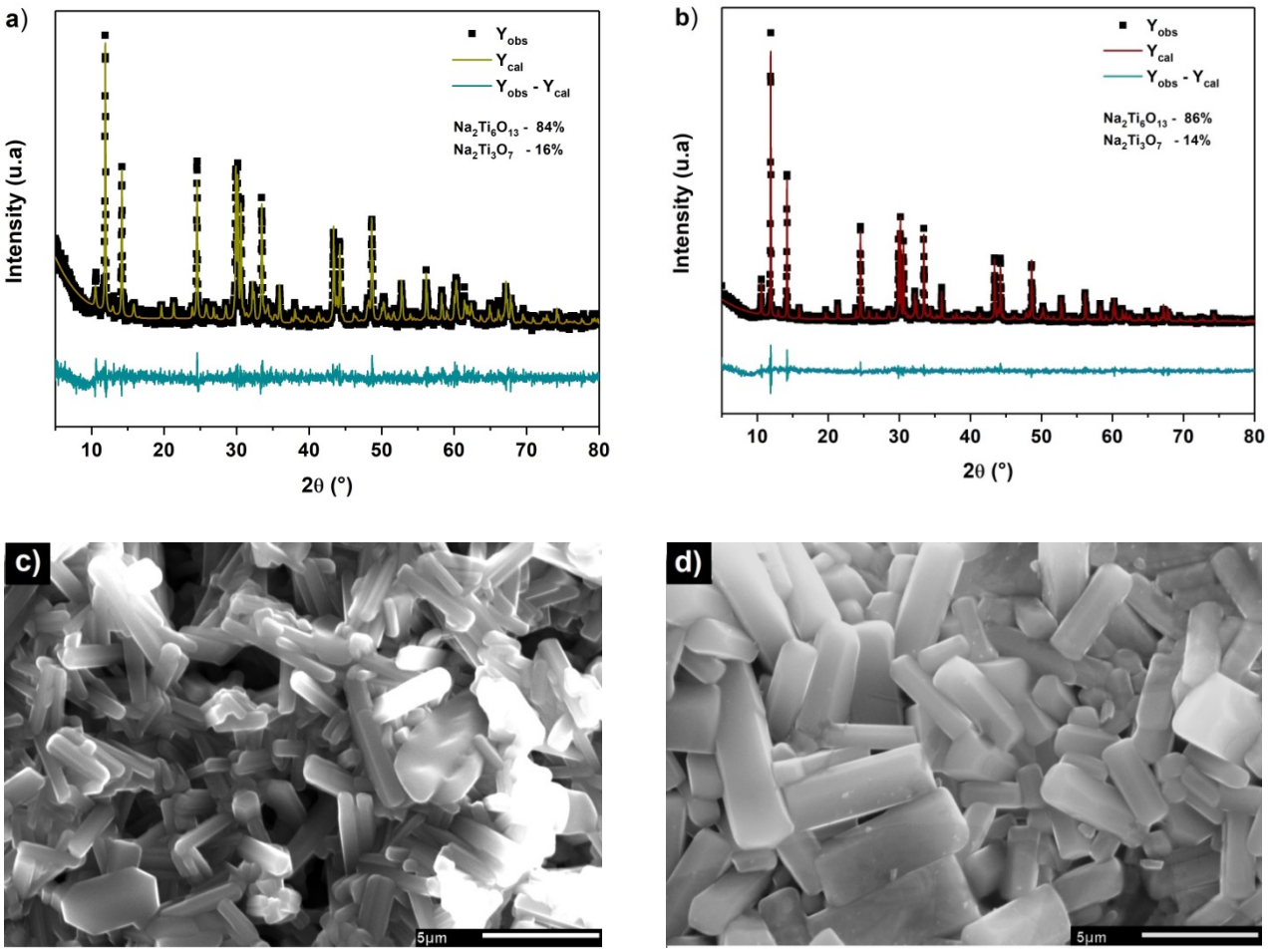

Figure 1 Rietveld refinement of the XRD data **of** a) conventionally sintered (NTF) and b) laser-sintered (NTL) $Na_2Ti_6O_{13}/Na_2Ti_3O_7$ ceramic samples. SEM images corresponding to each sample are shown in c) (NTF) and d) (NTL). Experimental (Y_{obs}) and theoretical (Y_{cal}) intensities as well as the residual lines ($Y_{obs} - Y_{cal}$) **of** both samples are shown. The phase composition of both samples is also reported in the figure.

The complex plane resistivity of each sample measured at room temperature (25°C) is shown in Figure 2. An appreciable difference between the diameters of the semicircles of the two samples can be observed. The semicircles were fitted using the circuit shown in Figure 2 to calculate the resistance (R) of each region, among other parameters. The grain resistivity (ρ_g), grain boundary resistivity (ρ_{gb}), and total resistivity ($\rho_t = \rho_g + \rho_{gb}$) can be calculated using the corresponding resistance value by considering the sample geometry.

Because the resistivity of the electrode/sample interface is considerably lower than the ρ_g and ρ_{bg} values, it was not considered.

NTL exhibited a semicircle with a smaller diameter and consequently a lower total resistivity (ρ_t = 0.145 MΩ·cm) than NTF (ρ_t = 1.93 MΩ·cm). Furthermore, a considerable decrease in the electrical resistivity of NTL was observed. Lower resistivity values result in higher conductivity, which is a desired property in materials for potential use in electronic applications, such as electrodes and solid-state electrolytes. The higher conductivity of NTL, which is caused by hopping p-type conduction [14, 26], can be associated with factors such as its higher relativity density, particle size, structural difference (as shown using the Rietiveld analysis), and processing conditions. In this context, NTL could show a long-range conductivity favored by the higher density, grains with more pronounced semiconductor characters, and a greater number of conductive paths. A similar behavior was also observed by Santos et al. [27] studying the production of mixed metal oxide anodes by laser heating. They observed a more compacted structure and reduced magnitude of the resistivity at room temperature in laser-produced anodes compared with conventionally fabricated anodes.

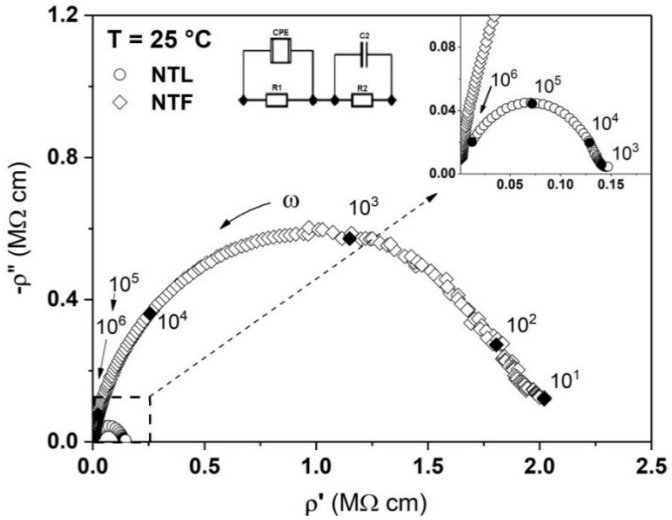

Figure 2 Complex resistivity plane of the sintered samples measured at 25°C. In these spectra, the white dots represent the experimental data and the numbers close to the black dots denote the frequency in Hz. The laser-sintered sample (NTL) shows a smaller-diameter semicircle than the conventionally sintered sample (NTF), achieving lower resistivity values. The equivalent electric circuit used to fit the experimental data is shown in the figure.

Figure 3 shows the logarithmic behavior of the total resistivity as a function of temperature. As the separation of grain and grain boundary contributions are not so clear, the total contribution was determined by the intersection of the curve with the real axis at low frequencies for each temperature. An anomalous increase in the resistivity values up to 75°C was observed, followed by a decrease in the resistivity when the temperature increase. This anomaly is reported as the PTCR behavior [22,23].

PTCR materials are commonly divided into four groups: polymer composites, ceramic composites, V_2O_3-based compounds, and $BaTiO_3$-based ceramics [22,23]. As a common characteristic, they show the existence of a transition temperature around which this effect occurs. Definitely, $Na_2Ti_6O_{13}$/$Na_2Ti_3O_7$-based materials do not show phase transition in this temperature region; thus, they do not fit in any one group. However, the studied samples exhibited obvious PTCR behaviors with a jump of three orders of magnitude, where NTL showed one order of magnitude less in the resistivity in the studied temperature range. To the best of our acknowledgment, the PTCR behavior in sodium titanate materials has not been reported before.

For the first time, Mächler. et al. [27] reported the effect of the addition of SiO_2 on the electrical properties of BNBT-based PTCR ceramics. Here, the authors achieved an increase of only one order of magnitude in the resistivity of the material [27]. Lakshmi K. et al. found that $BaTi_1$-$xSnxO_3$ samples (x = 0.07, 0.08, 0.09, and 0.1) exhibited a PTCR effect above TC in a temperature range that varies with the composition. Here, the values corresponding to the jump provide one-order resistivities [28]. Liang Y. et al. prepared Mn-doped BNT-BT-based PTCR materials. They demonstrated that Mn doping is an effective way for preparing high-performance, low-resistivity thermistors. Representative samples exhibited an extremely low resistivity of 6.3 Ωcm and high 3-order PTCR jump [29]. The

results presented here in terms of the PTCR effect are higher than those presented in the first two papers and similar to those achieved by Liang Y. et al.

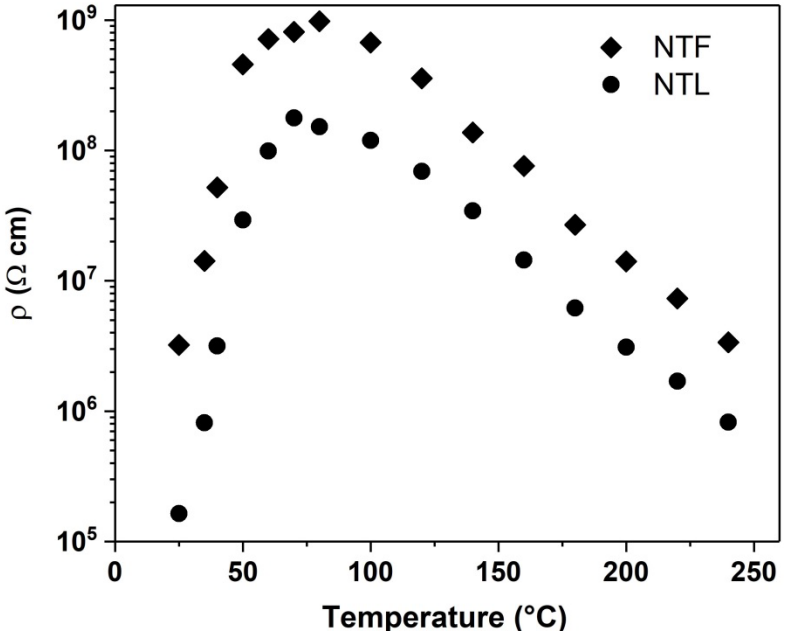

Figure 3 Temperature dependence of the resistivity **in** both conventionally sintered (NTF) and laser-sintered (NTL) $Na_2Ti_6O_{13}/Na_2Ti_3O_7$ ceramics. An abnormal increase of three orders of magnitude in the resistivity is displayed when the temperature rise from room temperature to approximately 75°C, revealing a noticeable PTCR effect.

The synergy between the two structures could be responsible for the manifestation of this apparently abnormal electrical response owing to the change in the mobility mechanism of charge carriers because of mixed phases. This behavior is schematically represented in Figure 4. The $Na_2Ti_6O_{13}$ phase (majority) shows a tunnel-shaped structure that favors the diffusion dynamics of charge p-type carriers [26]. While, the $Na_2Ti_3O_7$ shows a layered structure where three octahedrons of TiO_6 are joined by sharing their edges and forming short tapes that share their corners to form a zigzag litter $(Ti_3O_7)^{2-}$. This ion arrangement in the saw-teeth form caused great resistance and slow charge carrier migration. Moreover, this structure is known for having a high charge storage capacity [14].

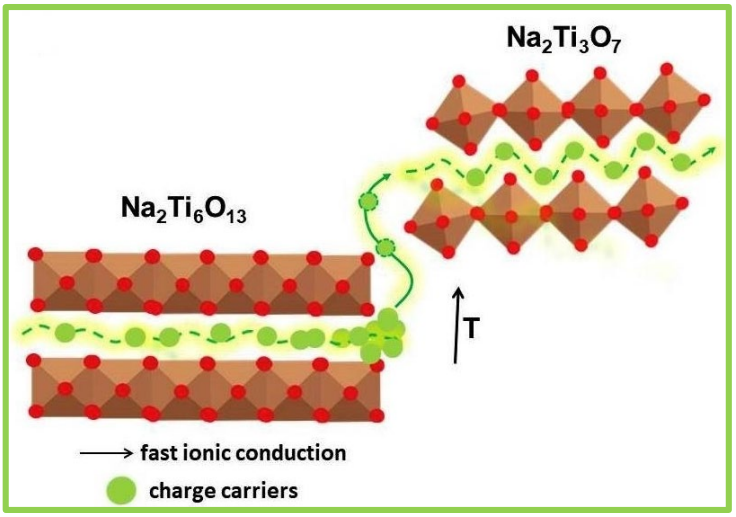

Figure 4 Schematic representation of the PTCR effect observed in the $Na_2Ti_6O_{13}/Na_2Ti_3O_7$ system. The charge carriers initially move through the tunnel-shaped structure of the $Na_2Ti_6O_{13}$ phase. When the temperature increases, they acquire sufficient energy to start a long-range conduction process until the thermal energy combined with the electric field becomes sufficient to restart the movement of the long-range charge carriers through the $Na_2Ti_3O_7$ structure.

Therefore, the charge carriers initially moved through the tunnel-shaped structure, rapidly decreasing the density of the charge carriers, which are retained by the lamellar structure. When the temperature increased, the charge carriers acquired sufficient energy to start a long-range conduction process through this structure, creating a "potential barrier" at the two phases interface; additional energy would be required for the conductive process to occur. Usually, additional energy is required for the charge carriers to overcome the potential barrier that is a combination between the rise of temperature and applied electric field. For temperatures above the value where the maximum resistivity is achieved (Figure 3), the thermal energy combined with the electric field becomes sufficient to restart the movement of the long-range charge carriers through the other structure, thereby justifying the increase in resistivity with temperature. Regarding this effect, the results are not conclusive and further studies will be required to clearly understand the mechanism inducing the outstanding PTCR response of this material.

Conclusion

In conclusion, the mixed phases of sodium titanate are obtained using both conventional and laser sintering methods. The phase compositions are evaluated using the Rietveld refinement of XRD data, indicating that no significant differences in the phase composition are observed because of the sintering process. However, the total resistivity value at room temperature shows a difference of an order of magnitude depending on the sintering process, which can be related to the observed difference in the structure and microstructure of the sintered samples. The temperature dependence of the electrical properties reveals an anomalous increase in resistivity with temperature. A growth of three orders of magnitude in the resistivity is observed in samples at temperatures between room temperature and approximately 75°C. This typical PTCR effect is observed for the first time in sodium titanate and to the best of our knowledge, in ceramic systems. A model based on the structural composition of $Na_2Ti_6O_{13}/Na_2Ti_3O_7$ system is proposed to explain the abnormal behavior of these materials.

Declaration of competing interest

The authors declare that they have no known competing financial interests or personal relationships that could have appeared to influence the work reported in this paper.

Acknowledgment

The authors would like to thank FAPEAM contract number 062.00939/2019 and FCT Portuguese agencies for the financial support, as well as to the National Institute of Amazon Researches (INPA) for their support by allowing the use of their facilities for electronic microscopy measurements performed in this work. This study was financed in part by the Coordenação de Aperfeiçoamento de Pessoal de Nível Superior - Brasil (CAPES) - Finance Code 001.

References

[1] Y. Xu, D. Bauer, M. Lübke, T.E. Ashton, Y. Zong, J.A. Darr, J. Power Sources. 408 (2018) 28–37.

[2] C.Y. Xu, J. Wu, P. Zhang, S.P. Hu, J.X. Cui, Z.Q. Wang, Y.D. Huang, L. Zhen, Cryst.Eng.Comm. 15 (2013) 3448–3454.

[3] Y. Leyet, F. Guerrero, J. Anglada-Rivera, R.F.B. de Souza, W.R. Brito, L. Aguilera, L.A. Pocrifka, R. Peña-Garcia, E. Padrón-Hernández, J. de la Cruz Pérez, J. Solid State Electrochem. 22 (2018) 1315–1319.

[4] Y.C. Chang, J.C. Lin, S.H. Wu, J. Alloys Compd. 749 (2018) 955–960.

[5] S.V.P. Vattikuti, P.A.K. Reddy, P.C. NagaJyothi, J. Shim, C. Byon, J. Alloys Compd. 740 (2018) 574–586.

[6] Z. Zhou, H. Xiao, F. Zhang, X. Zhang, Y. Tang, Electrochim. Acta. 211 (2016) 430–436.

[7] M. Xie, K. Wang, R. Chen, L. Li, F. Wu, Chem. Res. Chinese Univ. 31 (2015) 443–446.

[8] A.L. Sauvet, S. Baliteau, C. Lopez, P. Fabry, J. Solid State Chem. 177 (2004) 4508–4515.

[9] S. Chen, L. Gao, L. Zhang, X. Yang, Ionics (Kiel). 25 (2019) 2211–2219.

[10] H. Pan, X. Lu, X. Yu, Y.-S. Hu, H. Li, X.-Q. Yang, L. Chen, Adv. Energy Mater. 3 (2013) 1186–1194.

[11] N.G. Fagundes, F.X. Nobre, L.A.L. Basilio, A.D. Melo, B. Bandeira, J.C.C. Sales, J.C.S. Andrade, J. Anglada-Rivera, L. Aguilera, J. Pérez de la Cruz, Y. Leyet, Solid State Sci. 88 (2019) 63–66.

[12] Shripal, D. Maurya, Shalini, J. Kumar, Mater. Sci. Eng. B Solid-State Mater. Adv. Technol. 136 (2007) 5–10.

[13] S. Baliteau, A.L. Sauvet, C. Lopez, P. Fabry, Solid State Ionics. 178 (2007) 1517–1522.

[14] L. Aguilera, N. Fagundes, A.D. Melo, B. Bandeira, F.X. Nobre, J. Anglada-Rivera, J.P. Silva, J. Pérez de la Cruz, Y. Leyet, Ceram. Int. 46 (2020) 8706–8710.

[15] L.A.L. Basilio, F. Xavier, J.C.C.S. Jr, J.C.S. Andrade, J.A.- Rivera, L. Aguilera, R.S. Silva, J. Rodriguez-hernandez, J.P. De, Y. Leyet, Ceram. Int. 46 (2020) 23834–23839.

[16] C. Wang, W. Ping, Q. Bai, H. Cui, R. Hensleigh, R. Wang, A.H. Brozena, Z. Xu, J.

Dai, Y. Pei, C. Zheng, G. Pastel, J. Gao, X. Wang, H. Wang, J. Zhao, B. Yang, J. Luo, Y. Mo, B. Dunn, L. Hu, Science (80-.). 368 (2020) 521–526.

[17] Y. Leyet, F. Guerrero, J. Anglada-Rivera, D. Wilson, R. Peña-Garcia, A. Delgado, Y. Guerra, E. Padrón-Hernández, J. Pérez De La Cruz, Mater. Res. Express. 4 (2017) 045010.

[18] M. S. Silva, D. V. Sampaio, N. R. S. Souza, C. Kucera, J. Ballato, R. S. Silva, , J Electroceram. 42 (2019) 98–103.

[19] J.C.A. Santos, E.P. Silva, D. V Sampaio, D.C. Silva, N.R.S. Souza, C. Kucera, J. Ballato, R.S. Silva, J. Eur. Ceram. Soc. 40 (2020) 3673–3678.

[20] R.S. Silva, L.M. Jesus, T.C. Oliveira, D. V Sampaio, J.C.A. Santos, A.C. Hernandes, J. Eur. Ceram. Soc. 36 (2016) 4023–4030.

[21] L. Menezes, R. Santos, R. Raj, J.M. Peko, J. Alloys Compd. 682 (2016) 753–758.

[22] B. Huybrechts, K. Ishizaki, J Mat Sci. 30 (1995) 2463–2474.

[23] Y. Leyet, R. Peña, Y. Zulueta, F. Guerrero, J. Anglada-Rivera, Y. Romaguera, J.P. De La Cruz, Mater. Sci. Eng. B Solid-State Mater. Adv. Technol. 177 (2012) 832-837.

[24] C. Wu, W. Hua, Z. Zhang, B. Zhong, Z. Yang, G. Feng, W. Xiang, Z. Wu, X. Guo, Adv. Sci. 5 (2018) 1800519.

[25] D.O.S. Santos, V.M. Vasconcelos, S. Ronaldo, M.A. Rodrigo, K.I.B. Eguiluz, G.R. Salazar-banda, Electrochim Acta. 332 (2020) 135478.

[26] M. Dynarowska, J. Kotwiński, M. Leszczynska, M. Marzantowicz, F. Krok, Solid State Ionics. 301 (2017) 35–42.

[27] D. Mächler, J. Töpfer, Mater. Res. Bull. 89 (2017) 217–223.

[28] L. Kola, A. Bihari, M. Rath, M.S.R. Rao, P. Murugavel, Mater. Res. Bull. 106 (2018) 371–378.

[29] L. Yan, Q. Fu, D. Zhou, M. Wang, H. Zu, G. Wang, Z. Zheng, W. Luo, Ceram. Int. 45 (2019) 2185–2193.